Journal of Power Sources 239 (2013) 689–695

Contents lists available at SciVerse ScienceDirect

Journal of Power Sources

journal homepage: www.elsevier.com/locate/jpowsour

On-board state-of-health monitoring of lithium-ion batteries using linear parameter-varying models☆

Jürgen Remmlinger [a,*], Michael Buchholz [a], Thomas Soczka-Guth [b], Klaus Dietmayer [a]

[a] Institute of Measurement, Control and Microtechnology, Ulm University, Albert-Einstein-Allee 41, D-89081 Ulm, Germany
[b] Deutsche ACCUmotive GmbH & Co. KG, Neue Str. 95, D-73230 Kirchheim/Teck, Germany

HIGHLIGHTS

- ► Linear parameter-varying model valid in whole operation range of a hybrid vehicle.
- ► State-of-health (SOH) estimation based on internal resistance.
- ► Joint SOC/SOH estimation.
- ► Validation with real driving cycles.
- ► Validation with differently pre-aged cells.

ARTICLE INFO

Article history:
Received 14 September 2012
Received in revised form
19 November 2012
Accepted 21 November 2012
Available online 30 November 2012

Keywords:
Lithium-ion battery
State-of-health
LPV model
Internal resistance
Non-linear Kalman filter

ABSTRACT

This article presents a model-based monitoring approach for the internal resistance dependent state-of-health (SOH) of a high power lithium-ion battery cell used in hybrid electric vehicles. The monitoring method requires only signals which are already available in vehicles by measurement during regular driving. As varying battery temperatures occur during vehicle operation, a monitoring method has to cover the usual operation range from 0 °C to 50 °C. For this, a battery cell model from the class of linear parameter-varying (LPV) models is identified from measurement data. In contrast to many publications, the proposed monitoring method is validated using cell measurement data from driving cycles.

1. Introduction

In hybrid and electric vehicles, the key component influencing range and lifetime is the battery, which consists of lithium-ion battery cells in current and prospective vehicles. Since aging of the battery cells can occur within the battery lifetime on-board the vehicle, the current state of the cells is required for a short-term power prediction or an adaption of the long-term operation strategy, and also to detect possible failures or give the driver service advices. As the battery state is not measureable, it has to be monitored during operation.

Usually, the state-of-health (SOH) of a battery includes its actual battery capacity and its internal resistance. Thereby, the internal resistance determines the short- and mid-term overvoltages, whereas the capacity influences deviations in open-circuit voltage (OCV) due to charge and discharge. Aging related changes in internal resistance and capacity are not directly coupled, but usually point in the same direction. In this contribution, the change of the internal resistance is used for quantification of SOH.

Monitoring methods for on-board usage in a hybrid or electric vehicle have to fulfill specific requirements. Usually, no additional testing hardware or expensive sensors are available. Therefore, monitoring algorithms have to work with regular sensors used for battery operation and have to cope with their relatively high sample time and reduced accuracy. Recent surveys of proposed methods for this monitoring task can be found in [1–3].

Monitoring methods also differ in their computational complexity. Depending on the available computing power of the electronic control unit (ECU) of the battery management system (BMS), especially the availability of diagnosis information over

☆ This contribution was originally presented as a poster at UECT 2012.

* Corresponding author. Tel.: +49 731 50 26308.
E-mail address: juergen.remmlinger@uni-ulm.de (J. Remmlinger).

0378-7753/$ – see front matter © 2012 Elsevier B.V. All rights reserved.
http://dx.doi.org/10.1016/j.jpowsour.2012.11.102

operation time can be limited. Most monitoring methods determine the current SOH every sample time, i.e. each time a new set of measured values is captured. This causes a permanent computational load of the ECU, where the actual load depends on the complexity of the algorithms. The method in this paper also belongs to this group. A monitoring method which only occasionally provides an SOH update for specific signal intervals occurring during normal operation of the battery in a hybrid vehicle was already presented in [4], where the significantly reduced update rate of the SOH information (which might not be sufficient for all applications) yields a much lower computational requirement.

Driving an electric vehicle throughout the year, i.e. at varying ambient temperatures and with variable power demands, results in a broad operation range of battery cell temperatures. For an on-board monitoring method, it is most important to cover this temperature operation range to allow a permanent diagnosis update.

Known SOH monitoring methods either neglect this influence and are therefore limited to a small temperature range [5] or additionally estimate the electrical model [6–8], where the latter increases the computational load and makes it difficult to distinguish between aging effects and other influences like temperature changes. Therefore, with these methods, no tracking of the SOH over time in normal vehicle operation is possible. Furthermore, most presented methods in literature are not validated on measurement data relevant for vehicle operation, e.g. from driving cycles.

To enable a model-based monitoring method to determine an internal-resistance dependent SOH in the whole temperature operation range, the underlying cell model has to simultaneously describe both, temperature and aging dependent model changes. Evaluation tests verifying the applicability of such a monitoring method have to use measurement data from battery cells at different ambient and battery temperatures combined with different aging conditions of the battery cells.

In this contribution, a linear parameter-varying (LPV) electrical model of a battery cell is used to resolve this problem by covering the cells' non-linear behavior with varying temperatures. In general, LPV models (cf. e.g. [9] for an introduction to LPV models) offer advantages for a monitoring method as they are able to change their behavior according to a determining signal, the so-called scheduling signal, but still retain a linear characteristic if the scheduling signal remains constant.

In [10], a similar LPV model structure for battery cells has been proposed. There, charge direction and state-of-charge (SOC) were used as scheduling signals. Additionally, linear time-invariant (LTI) models were identified at some fixed temperatures and then combined to an LPV model. In contrast to this approach, temperature and aging are used as scheduling parameters for the LPV model in this contribution, and a direct LPV model identification is performed. This allows arbitrary varying temperatures within the identification data sets.

Based on this LPV model for the battery cells, a non-linear Kalman filter is used as an appropriate state and parameter estimation method. These estimates are derived from current, terminal cell voltage, and cell temperature measurements and include the SOH without explicitly calculating an internal resistance. An evaluation of this method is done using measurement data from lithium-ion power-cells pre-aged to different degrees. The measurements have been carried out on a test bench based on real driving cycles from a hybrid vehicle. The SOH values from the presented monitoring methods are validated using reference values determined during the measurements for evaluation.

The paper is organized as follows: Some theoretical background of the class of LPV systems is presented in Section 2. The derived model from this class suitable for on-board monitoring is presented in Section 3 and the monitoring method itself in Section 4. The contribution concludes with a summary in Section 5.

2. Linear parameter varying systems

Modeling non-linear systems for applications like model-based control or model-based diagnosis of systems always means a compromise between model accuracy and model complexity. For systems operated in one or a few distinct operation points, linearization of the non-linear system description at those operating points is a common means. Deriving a linear description of the system in every possible operation point leads to the LPV framework, where the linear system dynamics depend on the so-called scheduling parameter (or scheduling signal) defining the operation point of the system. A good overview on LPV modeling and identification can be found in [9].

Similar to LTI systems, there exist different representations of LPV models like input–output (IO) form or state-space (SS) models. This contribution is based on SS LPV models, and therefore models in IO form, like the LPV version of an autoregressive with exogenous inputs (ARX) model, are not further discussed. To be more precise, the time-discrete affine SS LPV innovation model form

$$\boldsymbol{x}(k+1) = \sum_{i=1}^{m} \mu_i(k)(\boldsymbol{A}_i\boldsymbol{x}(k) + \boldsymbol{B}_i\boldsymbol{u}(k)), \tag{1a}$$

$$\boldsymbol{y}(k) = \sum_{i=1}^{m} \mu_i(k)(\boldsymbol{C}_i\boldsymbol{x}(k) + \boldsymbol{D}_i\boldsymbol{u}(k)) \tag{1b}$$

is used here, where $\boldsymbol{x}\in\mathbb{R}^n$, $\boldsymbol{\mu} = [\mu_1 \quad \cdots \quad \mu_m]^{\mathrm{T}}\in\mathbb{R}^m$ with $\mu_1\equiv 1$, $\boldsymbol{u}\in\mathbb{R}^{n_u}$, and $\boldsymbol{y}\in\mathbb{R}^{n_y}$ denote the state vector, scheduling parameters, inputs, and outputs of the system, respectively. The system parameter matrices $\boldsymbol{A}_i$, $\boldsymbol{B}_i$, $\boldsymbol{C}_i$, and $\boldsymbol{D}_i$ can be interpreted as local linear models, where the scheduling parameters are the time-dependent local weights of the affine combination of those local linear models. The number of local linear models m is given by the number of scheduling parameters. For $m = 1$, system (1) simplifies to the standard LTI SS model.

LPV system (1) can also be regarded as a linear time-varying (LTV) system, where the time-varying system dynamic matrix is given as

$$\boldsymbol{A}(k) := \sum_{i=1}^{m} \mu_i(k)\boldsymbol{A}_i, \tag{2}$$

and the matrices $\boldsymbol{B}(k)$, $\boldsymbol{C}(k)$, and $\boldsymbol{D}(k)$ are defined analogously. The transition matrix of system (1) for j time steps starting at time step k is given by

$$\boldsymbol{\Phi}_j(k) = \boldsymbol{A}(k+j-1)\cdots\boldsymbol{A}(k+1)\boldsymbol{A}(k). \tag{3}$$

Instead of using time-variant parameter-matrices like above, the LPV system (1) can also be written with constant parameter matrices (with m times more columns):

$$\boldsymbol{x}(k+1) = \check{\boldsymbol{A}}\underbrace{(\boldsymbol{\mu}(k)\otimes\boldsymbol{x}(k))}_{=:\check{\boldsymbol{x}}(k)} + \check{\boldsymbol{B}}\underbrace{(\boldsymbol{\mu}(k)\otimes\boldsymbol{u}(k))}_{=:\check{\boldsymbol{u}}(k)}, \tag{4a}$$

$$\boldsymbol{y}(k) = \check{\boldsymbol{C}}\check{\boldsymbol{x}}(k) + \check{\boldsymbol{D}}\check{\boldsymbol{u}}(k). \tag{4b}$$

Here, the matrices $\check{\boldsymbol{B}}$, $\check{\boldsymbol{C}}$, and $\check{\boldsymbol{D}}$ are defined analogous to the definition of $\check{\boldsymbol{A}}$ given by

$$\check{\boldsymbol{A}} := [\boldsymbol{A}_1 \quad \boldsymbol{A}_2 \quad \cdots \quad \boldsymbol{A}_m]\in\mathbb{R}^{n\times mn}, \tag{5}$$

and $\otimes$ represents the Kronecker product (for a definition see e.g. [11]).

For many non-linear systems, the affine SS LPV form can be used as a valid model description or at least as a good approximation. For example, bilinear systems can be written in LPV affine form. An approximation of other non-linear systems can e.g. be done by a Taylor series expansion of the non-linear SS functions and an appropriate choice of the new LPV model state and scheduling signal [12].

3. Temperature and aging dependent cell model

As a basis for the monitoring method, in this section a temperature and aging dependent cell-model of the considered high-power lithium-ion cell is presented.

Although aging effects have considerable impact on the battery performance, the apparent influence on the measurable signals is low. This is demonstrated in Fig. 1, where the voltage signal of two cells is shown. The cells are of identical type, but differ significantly in internal resistance. The same current profile was applied to each cell at equal operation and initial battery conditions. From this small difference, the actual grade of degradation has to be detected. This is only possible with a model describing both the aging related changes of the behavior and the temperature influence at once.

For a model-based monitoring method, the terminal voltage of the battery has to be predicted with the knowledge of current input and cell temperature. Common cell models used for control and diagnosis applications are described in equivalent circuits (EC) [4]. The main parts of such an EC are an ideal voltage source, an ohmic resistor and several parallel connections of an ohmic resistor with a capacitor (*RC*). Thereby, the ideal voltage source represents the open circuit voltage. This is the normally SOC dependent voltage present at the cell terminal after appropriate long resting periods. The ohmic resistance and the *RC* elements describe the overvoltage occurring at the battery cell terminal while the battery is charged or discharged. For lithium-ion cells, the parameters of resistors and capacitors in the EC are depending on the cell temperature, the degradation of the cell, and the SOC. As this paper focuses on high-power lithium-ion cells for usage in a hybrid electric vehicle, the SOC dependence can be neglected, which means the model part describing the overvoltage is constant in the regarded SOC range at one temperature. This has been validated with measurements, where no SOC dependence of the battery cell characteristic could be observed within the limited SOC operation range of a hybrid electric vehicle, which depends on the operation strategy. Here, the SOC range is limited to 30–80%, as usual in hybrid electric vehicles.

In the following, the model part describing the overvoltage is referred to as the dynamic model part. This part is SOH dependent and described by an LPV model. The model is identified with data from different cells of the same type pre-aged to different SOHs. For identification of this model part, the OCV is subtracted from the measured terminal voltage to yield the required overvoltage. To be able to calculate the OCV, the SOC is calculated with the previously determined capacity during the test by current integration from a defined starting value. SOC determination by current integration is possible here, as the identification tests have been carried out on a test bench in the laboratory guaranteeing a precise current measurement. In this model, the current I is the input u and the overvoltage (the dynamic part of the voltage signal) U_{dyn} is the output y. Scheduling signals are the cell temperature T and the SOH. For model identification, the SOH scheduling signal is calculated from reference measurements at fixed temperatures as described in the following.

For a parameter identification of the SS LPV description (1) of the battery model, the knowledge of the states for each measured sample would be necessary. Therefore, an LPV transfer function is identified by a least-squares estimator (cf. e.g. [13]) and transformed to the SS model afterwards. As for every SS model with arbitrary states, the parameters of the identified aging and temperature dependent LPV model are unique except for a regular state transformation (cf. e.g. [14]). Nevertheless, the parameters in the direct-feedthrough matrix $\boldsymbol{D}$ are unique because they are not affected by state transformations and therefore have physical meaning. Due to the fact that the battery model is a single-input, single-output (SISO) model, the direct feedthrough reduces to a scalar parameter. A plot of the identified variation of this parameter over temperature is shown in Fig. 2.

A possible definition for the internal resistance dependent SOH is

$$\mathrm{SOH}_{Ri} = 1 + \frac{R_{\mathrm{i,ref}} - R_{\mathrm{i,actual}}}{R_{\mathrm{i,ref}}}. \tag{6}$$

The SOH_{Ri} value is usually given in percent, and both $R_{\mathrm{i,ref}}$ and $R_{\mathrm{i,actual}}$ refer to a fixed temperature, e.g room temperature. An SOH of zero usually means the state at end of life (EOL) of the battery, when degradation has led to a significant reduction of capacity or power capability. With this definition, SOH values over 100% and below 0% are possible. Hereby, an SOH of over 100% can especially occur for new cells which show a better performance than the nominal cell due to manufacturing variations. An SOH value below 0% is also possible in theory, but will usually not occur during operation due to a prior battery replacement. In the following, SOH always means the internal resistance dependent SOH, SOH_{Ri}.

To show the similar influence of temperature and SOH_{Ri} changes, the identified model is simulated with a current step input from a steady state for different temperatures and SOH_{Ri} values.

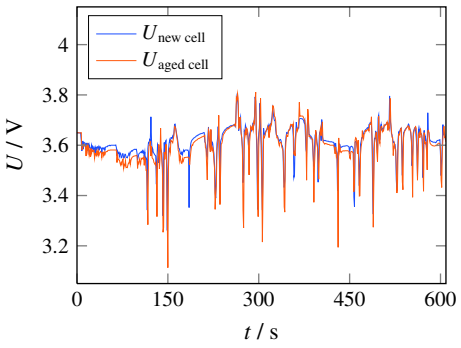

Fig. 1. Comparison of the measured voltage response of a new and an aged cell to the same current profile at the same ambient temperature.

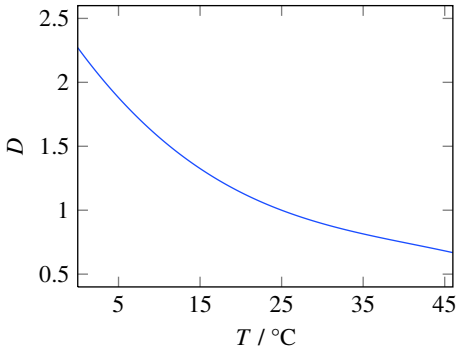

Fig. 2. Variation of the direct-feedthrough D of the identified LPV battery model over temperature.

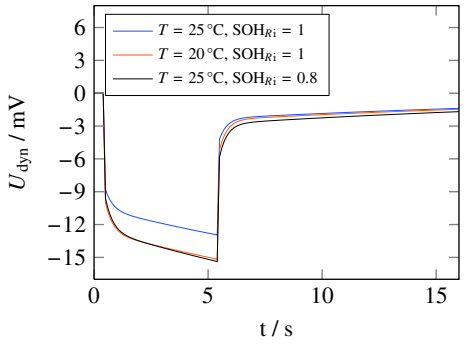

Fig. 3. Step responses of the model at different ambient temperature and SOH.

From Fig. 3 it can be seen that for the dynamic electric behavior an ambient temperature change from 20 °C to 25 °C is almost equivalent to a change of SOH_{Ri} from 1.0 to 0.8. This proves the already stated necessity of a combined temperature and aging dependent model for model-based SOH monitoring.

4. Realization and results of monitoring method

For the proposed monitoring approach, the LPV model of the battery cell was identified off-line from current and voltage measurements, as described in the previous section, at different temperatures and cell ages. The latter was achieved by carrying out the measurements with different cells of identical type, which previously have been aged to different degrees. In the following, the overall setup of the monitoring method is presented and the proposed method is validated with real driving cycles from hybrid vehicles which have been applied to the cells under laboratory conditions.

4.1. Central difference Kalman filter

Kalman filters are a commonly used means for state estimation. Here, a non-linear Kalman filter is necessary because of two reasons. Firstly, the OCV curve of the overall model (cf. Section 4.2) is a non-linear element, and secondly and even more important, the LPV model is only linear if temperature and SOH_{Ri} do not change. In general, LPV systems can also be seen as LTV systems. This would allow to use a linear Kalman filter. However, this is only correct if all scheduling parameters are measured signals or otherwise known. As one of the scheduling parameters, the SOH_{Ri}, has to be estimated in this contribution, this is not the case, and a non-linear Kalman filter is required.

For battery state estimation, several non-linear Kalman filters have been tested. These are essentially extended Kalman filters (EKF) ([6,15,16]) and unscented Kalman filters (UKF) [7,17,18], which belong to the class of sigma point Kalman filters (SPKF). SPKFs approximate the probability density of the state estimation with characteristic points, the so-called sigma points. In battery state estimation literature, it has been observed — as expected from theory [19] — that SPKFs perform better than EKFs. For complex non-linear systems, they even require less computational effort.

Therefore, a state estimation with a central difference Kalman filter (CDKF) is performed based on the proposed cell model. The CDKF is also from the class of SPKFs. In comparison to the commonly used UKF, the CDKF shows an equal estimation performance in all practical purposes but has the advantage of a lower parameter count of the algorithm [19]. A description of the used CDKF algorithm is given in the Appendix A.

4.2. Setup of the model used for on-board diagnosis

For identification, the SOC dependent OCV has been subtracted from the terminal voltage. To complete the model for terminal voltage prediction, the SOC of the cell is added to the state vector. In the output equation, the SOC is converted into the corresponding OCV with a static characteristic.

Furthermore, the SOH_{Ri} is added to the state vector to estimate it in a so-called joint estimation, i.e. system states like SOC and system parameters like SOH_{Ri} are processed together in one CDKF at the same time. This allows the SOH_{Ri} to be estimated from the input and output measurements directly without explicitly estimating the internal resistance. The second scheduling signal beside SOH_{Ri} is the cell temperature. The temperature is measured with a temperature sensor at the cell surface and handed over to the cell model. This results in the following filter inputs, outputs, states, and relation for the scheduling parameter in the included LPV model:

$$\boldsymbol{x} = \begin{bmatrix} \boldsymbol{x}_{U_{\mathrm{dyn}}} \\ \mathrm{SOC} \\ \mathrm{SOH}_{Ri} \end{bmatrix},$$
$$u = I,$$
$$y = U_{\mathrm{t}},$$
$$\mu = f(T, \mathrm{SOH}_{Ri}).$$

The filter setup is illustrated in Fig. 4. A current which is requested by the power electronics is drawn from the battery and leads to a voltage change at the cell terminals. Furthermore, due to the power losses and in combination with the ambient temperature, a temperature change of the cell occurs. The filter operates

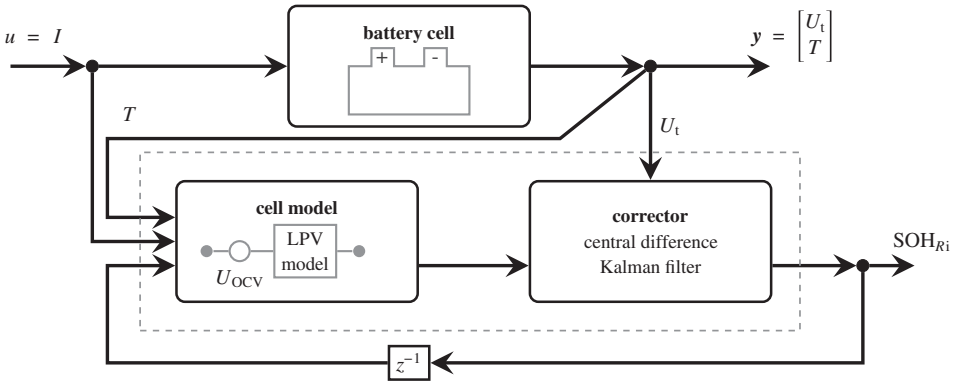

Fig. 4. Illustration of the monitoring algorithm in a block diagram.

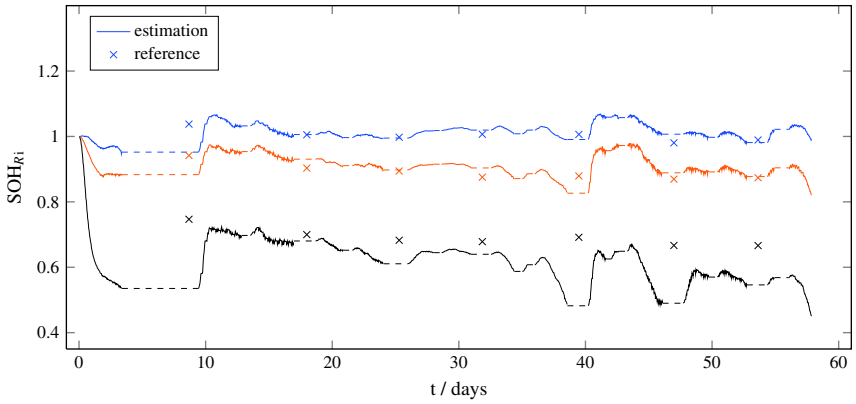

Fig. 5. SOH estimation of three cells (blue new, red degraded, black old) under the same current profile applied. (For interpretation of the references to colour in this figure legend, the reader is referred to the web version of this article.)

recursively and in parallel to the real battery cell. Thereby, the underlying cell model is simulated with the measured cell current as an input and the measured cell temperature as well as the estimated SOH$_{Ri}$ from the state vector as scheduling parameters for the included LPV model. The cell model predicts a terminal voltage which is compared to the measured terminal voltage in the corrector of the filter. If deviations occur, the filter states including SOC and SOH$_{Ri}$ are adapted. The filter states are finally used as initial values for the simulation in the next filter step.

4.3. Monitoring results

To validate the presented method in a setup as close as possible to a vehicle on-board application, recorded data from driving a hybrid vehicle was transferred to a laboratory battery testing system by setting the measured current as current demand for the testing. This has the advantage that for validation purposes, a regular determination of the degradation with a common test is possible. Here, this was done by applying high-current pulse profiles to the battery cells at room-temperature in a steady state after a long resting period.

The recorded driving cycles from a hybrid vehicle have been applied to all cells at the same varying temperatures. Tests have been carried out in a temperature chamber allowing precise adjustment of the ambient temperature. The applied current profiles at each different ambient temperature value were selected according to the temperature at which they occurred in the vehicle. Thus, it was possible to ensure only current demands were requested which the BMS would allow at this operation point. The diagnosis method was only applied during the driving profiles but not during reference tests to guarantee realistic conditions for an evaluation of the on-board method.

The SOH$_{Ri}$ values estimated through the monitoring method are compared to intermediate reference measurements in Fig. 5 for a duration of about 8 weeks for three differently pre-aged cells. It can be seen that the estimation matches the reference well after a short initialization phase. The estimates allow not only to distinguish between the three pre-aged cells but also follow the degradation during the test time, especially obvious for the most aged cell plotted in black.

For the most aged cell, there also occur some abrupt changes in the estimation at 38 and 45 days. This cell shows not only a high internal resistance, but also a significant capacity loss. Hence, for some driving profiles, the SOC reaches small values compared to the other cells. In these cases, the terminal voltage drops to very low values what leads to underestimation of the SOH$_{Ri}$. To avoid

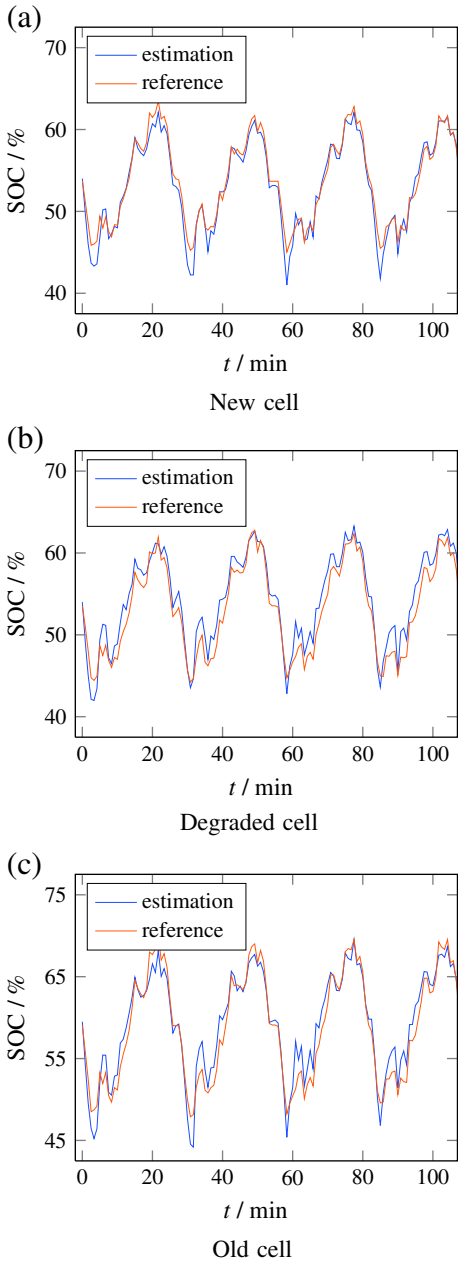

Fig. 6. SOC estimation as a byproduct of SOH estimation.

Table 1
SOC estimation error of differently pre-aged cells in the profile plotted in Fig. 6.

SOC/%	Mean of error	Variance of error
New cell	0.55	1.25
Degraded cell	−1.29	1.70
Old cell	−0.55	3.22

these relatively fast changes of the estimates, an appropriate low-pass or moving-average filter could be used.

Besides the SOH_{Ri} estimation, also an accurate SOC estimation is performed automatically by the proposed method due to the added internal SOC state in the filter state vector. Although the pre-aged cells in the test do not only differ in their SOH_{Ri}, but also in their capacities, and the capacity value used in the filter model was fixed at the default value for a new cell, a reliable SOC determination is possible. For a new cell, a degraded cell, and an old cell, the SOC estimates are presented in Fig. 6, and mean as well as variance of the SOC estimation error are given in Table 1. It can be seen that for the old cell the variance of the estimation error is slightly higher but still remains in a very good range. The reference SOC in this comparison was calculated through current integration with the actual capacity values also determined through regular intermediate tests.

5. Conclusions

For the proposed monitoring method, the SOH of a lithium-ion battery cell is represented by the changes in its internal resistance during aging leading to changes in its dynamic electrical model. This model is an LPV model covering the temperature operation range of battery cells in a hybrid electric vehicle. The model is used in a non-linear Kalman filter to estimate SOH and SOC on-line from on-board measurements continuously. The proposed method was validated on measurement data from real driving cycles and showed good results. If a comparable model based SOC determination method is used anyway, the additional effort for SOH_{Ri} estimation is low and yields good estimates of the actual degree of degradation.

As a precise SOC estimation is possible with the presented method, which is a basis for capacity estimation, an analysis of possible extensions for this task will be investigated in future work. This would allow to estimate a capacity related SOH, which would complete the diagnosis task for battery cells in combination with the presented SOH estimation related to the internal resistance.

Appendix A. Algorithm of the central difference Kalman filter

The following description of the algorithm follows the one given in [20]. A detailed derivation of SPKFs can also be found in [19]. As all Kalman filters, a CDKF works with a predictor-corrector structure. In the time update step, the model-based predictor calculates a state vector $\hat{x}_{k+1}^-$ (model simulation for one time step), which is corrected with measurements from the observed system in the measurement update to $\hat{x}_{k+1}^+$. The time update equation $\mathbf{f}(\cdot)$ and measurement update equation $\mathbf{g}(\cdot)$ are evaluated $i = 2n + 1$ times (where n is the model order) in the so-called sigma points $\chi_{i,k+1}$ to approximate the non-linearities.

Initialization:

$$\hat{\boldsymbol{x}}_{\boldsymbol{0}} = \mathrm{E}\{\boldsymbol{x}_{\boldsymbol{0}}\}$$
$$\boldsymbol{S}_{\boldsymbol{x},\boldsymbol{0}} = \mathrm{chol}\left\{\mathrm{E}\left\{(\boldsymbol{x}_{\boldsymbol{0}} - \hat{\boldsymbol{x}}_{\boldsymbol{0}})(\boldsymbol{x}_{\boldsymbol{0}} - \hat{\boldsymbol{x}}_{\boldsymbol{0}})^{\mathrm{T}}\right\}\right\}$$

Calculation of sigma points for time update:

$$\chi_{\boldsymbol{0},\boldsymbol{k+1}}^- = \hat{\boldsymbol{x}}_{\boldsymbol{k}}^+$$
$$\chi_{\boldsymbol{i},\boldsymbol{k+1}}^- = \hat{\boldsymbol{x}}_{\boldsymbol{k}}^+ + h(\boldsymbol{S}_{\boldsymbol{x},\boldsymbol{k}}^+)_{:,i}$$
$$\chi_{\boldsymbol{i+n},\boldsymbol{k+1}}^- = \hat{\boldsymbol{x}}_{\boldsymbol{k}}^+ - h(\boldsymbol{S}_{\boldsymbol{x},\boldsymbol{k}}^+)_{:,i}$$

Time update:

$$\chi_{\boldsymbol{i},\boldsymbol{k+1}}^{\boldsymbol{p}} = \mathbf{f}(\chi_{\boldsymbol{i},\boldsymbol{k+1}}^-, \boldsymbol{u}_k, \boldsymbol{0})$$
$$\hat{\boldsymbol{x}}_{\boldsymbol{k+1}}^- = \frac{h^2 - n}{h^2}\chi_{\boldsymbol{0},\boldsymbol{k+1}}^{\boldsymbol{p}} + \frac{1}{2h^2}\sum_{i=1}^{2n}\chi_{\boldsymbol{i},\boldsymbol{k+1}}^{\boldsymbol{p}}$$
$$\boldsymbol{S}_{\boldsymbol{x}}^{(1)} = \frac{1}{2h}\left\{\chi_{\boldsymbol{i},k+1}^{\boldsymbol{p}} - \chi_{\boldsymbol{i+n},\boldsymbol{k+1}}^{\boldsymbol{p}}\right\}_{i=1,\ldots,n}$$
$$\boldsymbol{S}_{\boldsymbol{x}}^{(2)} = \frac{\sqrt{\sigma_4 - 1}}{2h^2}\left\{\chi_{i,k+1}^{p} + \chi_{i+n,k+1}^{p} - 2\chi_{0,k+1}^{p}\right\}_{i=1,\ldots,n}$$
$$\boldsymbol{S}_{\boldsymbol{x},\boldsymbol{k+1}}^- = \mathrm{QR}\{(\boldsymbol{S}_{\boldsymbol{x}}^{(1)} \quad \boldsymbol{S}_{\boldsymbol{x}}^{(2)} \quad \sqrt{\boldsymbol{Q}_{\boldsymbol{w}}})\}$$

Calculation of sigma points for measurement update:

$$\chi_{\boldsymbol{0},\boldsymbol{k+1}}^+ = \hat{\boldsymbol{x}}_{\boldsymbol{k+1}}^-$$
$$\chi_{\boldsymbol{i},\boldsymbol{k+1}}^+ = \hat{\boldsymbol{x}}_{\boldsymbol{k+1}}^- + h(\boldsymbol{S}_{\boldsymbol{x},\boldsymbol{k+1}}^-)_{:,i}$$
$$\chi_{\boldsymbol{i+n},\boldsymbol{k+1}}^+ = \hat{\boldsymbol{x}}_{\boldsymbol{k+1}}^- - h(\boldsymbol{S}_{\boldsymbol{x},\boldsymbol{k+1}}^-)_{:,i}$$

Measurement update:

$$\mathcal{Y}_{\boldsymbol{i},\boldsymbol{k}} = \boldsymbol{g}(\chi_{\boldsymbol{i},\boldsymbol{k+1}}^+, \boldsymbol{u}_k, 0)$$
$$\hat{\boldsymbol{y}}_{\boldsymbol{k+1}}^- = \frac{h^2 - n}{h^2}\mathcal{Y}_{\boldsymbol{0},\boldsymbol{k}} + \frac{1}{2h^2}\sum_{i=1}^{2n}(\mathcal{Y}_{\boldsymbol{i},\boldsymbol{k}})$$
$$\boldsymbol{S}_{\boldsymbol{y}}^{(1)} = \frac{1}{2h}\left\{(\mathcal{Y}_{\boldsymbol{i},\boldsymbol{k}} - \mathcal{Y}_{\boldsymbol{i+n},\boldsymbol{k}})\right\}_{i=1,\ldots,n}$$
$$\boldsymbol{S}_{\boldsymbol{y}}^{(2)} = \frac{\sqrt{\sigma_4 - 1}}{2h^2}\left\{(\mathcal{Y}_{\boldsymbol{i},\boldsymbol{k}} + \mathcal{Y}_{\boldsymbol{i+1},\boldsymbol{k}} - 2\mathcal{Y}_{\boldsymbol{0},\boldsymbol{k}})\right\}_{i=1,\ldots,n}$$
$$\boldsymbol{S}_{\boldsymbol{y},\boldsymbol{k+1}}^- = \mathrm{QR}\{(\boldsymbol{S}_{\boldsymbol{y}}^{(1)} \quad \boldsymbol{S}_{\boldsymbol{y}}^{(2)} \quad \sqrt{\boldsymbol{R}_{\boldsymbol{w}}})\}$$
$$\hat{\boldsymbol{P}}_{\boldsymbol{xy},\boldsymbol{k+1}}^- = \boldsymbol{S}_{\boldsymbol{x},\boldsymbol{k+1}}^-(\boldsymbol{S}_{\boldsymbol{y}}^{(1)})^{\mathrm{T}}$$
$$\boldsymbol{K}_{\boldsymbol{k+1}} = \hat{\boldsymbol{P}}_{\boldsymbol{xy},\boldsymbol{k+1}}^-(\boldsymbol{S}_{\boldsymbol{y},\boldsymbol{k+1}}^-\boldsymbol{S}_{\boldsymbol{y},\boldsymbol{k+1}}^{-\mathrm{T}})^{-1}$$
$$\hat{\boldsymbol{x}}_{\boldsymbol{k+1}}^+ = \hat{\boldsymbol{x}}_{\boldsymbol{k+1}}^- + \boldsymbol{K}_{\boldsymbol{k+1}}(\boldsymbol{y}_{\boldsymbol{k+1}} - \hat{\boldsymbol{y}}_{\boldsymbol{k+1}}^-)$$
$$\boldsymbol{S}_{\boldsymbol{x},\boldsymbol{k+1}}^+ = \mathrm{QR}\{(\boldsymbol{S}_{\boldsymbol{x},\boldsymbol{k+1}}^- - \boldsymbol{K}_{\boldsymbol{k+1}}\boldsymbol{S}_{\boldsymbol{y}}^{(1)} \quad \boldsymbol{K}_{\boldsymbol{k+1}}\boldsymbol{S}_{\boldsymbol{y}}^{(2)} \quad \boldsymbol{K}_{\boldsymbol{k+1}}\sqrt{\boldsymbol{R}_{\boldsymbol{w}}})\}$$

References

[1] J. Remmlinger, M. Buchholz, K. Dietmayer, Methods for monitoring the state of batteries in automotive applications, in: VDE Verlag (Ed.), VDE-Kongress EMobility, 2010.
[2] J. Zhang, J. Lee, A review on prognostics and health monitoring of Li-ion battery, Journal of Power Sources 196 (2011) 6007–6014.
[3] K.B. Hatzell, A. Sharma, H.K. Fathy, Survey of long-term health modeling, estimation, and control of lithium-ion batteries: challenges and opportunities, in: American Control Conference (ACC) 2012.
[4] J. Remmlinger, M. Buchholz, M. Meiler, P. Bernreuter, K. Dietmayer, State-of-health monitoring of lithium-ion batteries in electric vehicles by on-board internal resistance estimation, Journal of Power Sources 196 (2011) 5325–5331.
[5] B.S. Bhangu, P. Bentley, D.A. Stone, C.M. Bingham, State-of-charge and state-of-health prediction of lead-acid batteries for hybrid electric vehicles using non-linear observers, in: Proc. 11th European Conference on Power Electronics and Applications, 2005.

[6] G.L. Plett, Extended Kalman filtering for battery management systems of LiPB-based HEV battery packs part 3. State and parameter estimation, Journal of Power Sources 134 (2004) 277–292.
[7] F. Zhang, G. Liu, L. Fang, Battery state estimation using unscented Kalman filter, in: IEEE International Conference on Robotics and Automation 2009. ICRA '09, 2009, pp. 1863–1868.
[8] I.-S. Kim, A technique for estimating the state of health of lithium batteries through a dual-sliding-mode observer, IEEE Transactions on Power Electronics 25 (2010) 1013–1022.
[9] R. Tóth, Modeling and Identification of Linear Parameter-Varying Systems, Springer, Berlin, 2010.
[10] Y. Hu, S. Yurkovich, Linear parameter varying battery model identification using subspace methods, Journal of Power Sources 196 (2011) 2913–2923.
[11] J.W. Brewer, Kronecker products and matrix calculus in system theory, IEEE Transactions on Circuit and Systems 25 (9) (1978) 772–781.
[12] W.E. Larimore, M. Buchholz, ADAPT-LPV software for identification of nonlinear parameter-varying systems, in: Proceedings of the 16th IFAC Symposium on System Identification (SYSID 2012) 2012, pp. 1820–1825.
[13] L. Ljung, System Identification: Theory for the User, second ed., Prentice Hall, Upper Saddle River, 1999.
[14] M. Buchholz, Subspace-Identification zur Modellierung von PEM-Brennstoffzellen-Stacks, In: Schriften des Instituts für Regelungs- und Steuerungssysteme, vol. 07, Karlsruher Institut für Technologie, KIT Scientific Publishing, Karlsruhe, 2010.
[15] G.L. Plett, Extended Kalman filtering for battery management systems of LiPB-based HEV battery packs part 1. Background, Journal of Power Sources 134 (2004) 252–261.
[16] G.L. Plett, Extended Kalman filtering for battery management systems of LiPB-based HEV battery packs part 2. Modeling and identification, Journal of Power Sources 134 (2004) 262–276.
[17] G.L. Plett, Sigma-point Kalman filtering for battery management systems of LiPB-based HEV battery packs part 1: introduction and state estimation, Journal of Power Sources 161 (2006) 1356–1368.
[18] G.L. Plett, Sigma-point Kalman filtering for battery management systems of LiPB-based HEV battery packs part 2: Simultaneous state and parameter estimation, Journal of Power Sources 161 (2006) 1369–1384.
[19] R. van der Merwe, Sigma-point Kalman filters for probabilistic inference in dynamic state-space models, Ph.D. thesis, Oregon Health & Science University, 2004.
[20] J. Fox, Robotergestützte Parameterschätzung für inertiale Messsysteme, Logos Verlag, Berlin, 2007.